

Pentadienyl-Metal-Phosphine Chemistry. 9.¹ The 2,4-Dimethylpentadienyl-Iron-Trimethylphosphine Reaction System

John R. Bleeke* and Mary K. Hays

Department of Chemistry, Washington University, St. Louis, Missouri 63130

Received May 31, 1986

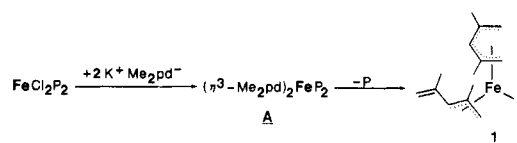
The reaction of $\text{FeCl}_2(\text{PMe}_3)_2$ with potassium 2,4-dimethylpentadienide-tetrahydrofuran ($\text{K}^+2,4\text{-Me}_2\text{pd}^-$) can be directed into three separate manifolds by varying the ratio of $\text{K}^+2,4\text{-Me}_2\text{pd}^-$ to iron. Use of a 2:1 $\text{K}^+2,4\text{-Me}_2\text{pd}^-:\text{Fe}$ ratio leads to the production of $(\eta^5\text{-}2,4\text{-Me}_2\text{pd})(\eta^3\text{-}2,4\text{-Me}_2\text{pd})\text{Fe}(\text{PMe}_3)$ (1) while a 1:1 $\text{K}^+2,4\text{-Me}_2\text{pd}^-:\text{Fe}$ ratio yields $(\eta^4\text{-isopropenyltrimethylenemethyl})\text{Fe}(\text{PMe}_3)_3$ (2) via a reaction sequence involving activation of a C-H bond in a 2,4-Me₂pd methyl group. When the ratio of $\text{K}^+2,4\text{-Me}_2\text{pd}^-:\text{Fe}$ is reduced to 1:2, $(\eta^5\text{-}2,4\text{-Me}_2\text{pd})\text{Fe}(\text{PMe}_3)_3^+\text{FeCl}_3(\text{PMe}_3)^-$ (3) is produced. Single-crystal X-ray diffraction studies of both 2 and 3 have been carried out. Compound 2 crystallizes in the monoclinic space group $P2_1/c$ with $a = 8.878$ (1) Å, $b = 14.737$ (4) Å, $c = 16.689$ (3) Å, $\beta = 102.25$ (1)°, $V = 2129.5$ (8) Å³, and $Z = 4$. The complex assumes an approximate octahedral geometry with C1, C3, and C6 of the isopropenyltrimethylenemethyl ligand (iTMM) and the three phosphine phosphorus atoms occupying the six coordination sites. The iTMM ligand exhibits an umbrella shape with C2 bent out of the C1/C3/C6 plane. Compound 3 crystallizes in the monoclinic space group $C2/c$ with $a = 18.442$ (5) Å, $b = 18.433$ (5) Å, $c = 17.875$ (5) Å, $\beta = 91.87$ (2)°, $V = 6073$ (3) Å³, and $Z = 8$. The coordination geometry of the cation is approximately octahedral with C1, C3, and C5 of the 2,4-Me₂pd ligand and P1, P2, and P3 of the PMe_3 ligands occupying the six coordination sites. The anion of 3, $\text{FeCl}_3(\text{PMe}_3)^-$, adopts an ethane-like geometry with the three chloro ligands on iron and the three methyl groups on phosphorus arranged in a staggered orientation. The reaction of 1 with HO_3SCF_3 and 2 equiv of PMe_3 in diethyl ether produces $(\eta^5\text{-}2,4\text{-Me}_2\text{pd})\text{Fe}(\text{PMe}_3)_3^+\text{O}_3\text{SCF}_3^-$ (4). In solution, the $\eta^5\text{-}2,4\text{-Me}_2\text{pd}$ ligand in 4 rotates with respect to the $\text{Fe}(\text{PMe}_3)_3$ fragment. Line-shape simulations of the variable-temperature $^{31}\text{P}\{^1\text{H}\}$ NMR spectra have enabled us to calculate a ΔG^\ddagger of 11.5 ± 0.5 kcal for this process.

Introduction

Electron-rich organometallic complexes containing hydrocarbon ligands have recently attracted a great deal of attention because of their ability to react with bonds that are normally difficult to activate² and their ability to stabilize unusual bonding interactions such as three-center C-H-M interactions.³ In addition, compounds of this class can undergo oxidation quite readily and the chemistry of the resulting radical species is often interesting.⁴

Our efforts in this area have focused on synthesizing and studying the reaction chemistry of transition-metal-phosphine complexes containing the acyclic pentadienyl ligand (pd). These are highly electron-rich molecules whose reactivity is further enhanced by the accessibility of a variety of pd-bonding modes (η^5 , η^3 , and η^1).⁵

Scheme I



Earlier, we reported that the reaction of $\text{FeCl}_2(\text{PMe}_3)_2$ ⁶ with 2 equiv of potassium pentadienide-tetrahydrofuran (K^+pd^-)⁷ produced $(\eta^3\text{-pd})_2\text{Fe}(\text{PMe}_3)_2$ in high yield.^{1b} We now report that the replacement of K^+pd^- with its 2,4-dimethylpentadienyl analogue, $\text{K}^+2,4\text{-Me}_2\text{pd}^-$,⁷ in the above reaction system leads to very different chemistry. In fact, by varying the conditions, we are able to direct this reaction into three separate manifolds.

Results and Discussion

A. Manifolds for the Reaction of $\text{FeCl}_2(\text{PMe}_3)_2$ with Potassium 2,4-Dimethylpentadienide-Tetrahydrofuran. As shown in Figure 1, the course of the reaction of $\text{FeCl}_2(\text{PMe}_3)_2$ ⁶ with potassium 2,4-dimethylpentadienide-tetrahydrofuran⁷ changes dramatically upon varying the $\text{K}^+2,4\text{-Me}_2\text{pd}^-$ to iron ratio. Use of a 2:1 $\text{K}^+2,4\text{-Me}_2\text{pd}^-:\text{FeCl}_2(\text{PMe}_3)_2$ ratio leads to the production of $(\eta^5\text{-}2,4\text{-Me}_2\text{pd})(\eta^3\text{-}2,4\text{-Me}_2\text{pd})\text{Fe}(\text{PMe}_3)$ (1). However, when equimolar quantities of $\text{K}^+2,4\text{-Me}_2\text{pd}^-$ and $\text{FeCl}_2(\text{PMe}_3)_2$ are employed, the reaction is diverted into the central manifold in Figure 1, which results in the synthesis of $(\eta^4\text{-iTMM})\text{Fe}(\text{PMe}_3)_3$ (2) where "iTMM" is our abbreviation for the isopropenyl-substituted trimethylenemethyl ligand. Finally, reduction of the $\text{K}^+2,4\text{-Me}_2\text{pd}^-:\text{FeCl}_2$ -

(1) The previous papers in this series are: (a) Bleeke, J. R.; Kotyk, J. *J. Organometallics* 1983, 2, 1263. (b) Bleeke, J. R.; Hays, M. K. *Ibid.* 1984, 3, 506. (c) Bleeke, J. R.; Peng, W.-J. *Ibid.* 1984, 3, 1422. (d) Bleeke, J. R.; Kotyk, J. J. *Ibid.* 1985, 4, 194. (e) Bleeke, J. R.; Peng, W.-J. *Ibid.* 1986, 5, 635. (f) Bleeke, J. R.; Stanley, G. G.; Kotyk, J. J. *Ibid.* 1986, 5, 1642. (g) Bleeke, J. R.; Moore, D. A. *Inorg. Chem.* 1986, 25, 3522. (h) Bleeke, J. R.; Donaldson, A. J. *Organometallics* 1986, 5, 2401.

(2) See, for example: (a) Janowicz, A. H.; Bergman, R. G. *J. Am. Chem. Soc.* 1983, 105, 3929. (b) Jones, W. D.; Feher, F. *Ibid.* 1984, 106, 1650. (c) Bergman, R. G.; Seidler, P. F.; Wenzel, T. T. *Ibid.* 1985, 107, 4358. (d) Green, M. L. H.; Joyner, D. S.; Wallis, J.; Bell, J. P. 190th National Meeting, American Chemical Society, Chicago, IL (Sept. 1985).

(3) See, for example: (a) Ittel, S. D.; Van-Catledge, F. A.; Jesson, J. P. *J. Am. Chem. Soc.* 1979, 101, 6905. (b) Schultz, A. J.; Brown, R. K.; Williams, J. M.; Schrock, R. *Ibid.* 1981, 103, 169. (c) Dawoodi, Z.; Green, M. L. H.; Mtetwa, V. S. B.; Prout, K. *J. Chem. Soc., Chem. Commun.* 1982, 1410. (d) Cracknell, R. B.; Orpen, A. G.; Spencer, J. L. *Ibid.* 1984, 326. (e) Brookhart, M.; Green, M. L. H. *J. Organomet. Chem.* 1983, 250, 395 and references cited therein.

(4) See, for example: (a) Hayes, J. C.; Cooper, N. J. *J. Am. Chem. Soc.* 1982, 104, 5570. (b) Harlow, R. L.; McKinney, R. J.; Witney, J. F. *Organometallics* 1983, 2, 1839. (c) Reference 1e.

(5) See papers cited in ref 1. See also: (a) Paz-Sandoval, M. A.; Powell, P.; Drew, M. G. B.; Perutz, R. N. *Organometallics* 1984, 3, 1026. (b) Ernst, R. D. *Acc. Chem. Res.* 1985, 18, 56 and references cited therein.

(6) Harris, T. V.; Rathke, J. W.; Muettterties, E. L. *J. Am. Chem. Soc.* 1978, 100, 6966.

(7) Yasuda, H.; Ohnuma, Y.; Yamauchi, M.; Tani, H.; Nakamura, A. *Bull. Chem. Soc. Jpn.* 1979, 52, 2036.

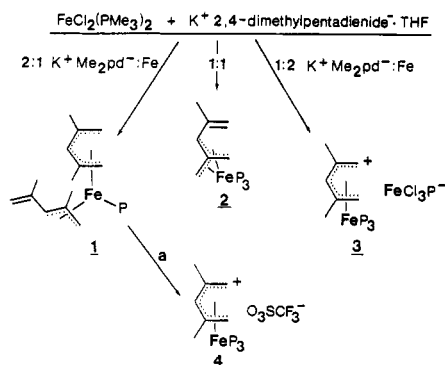
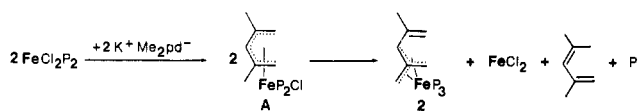


Figure 1. Manifolds for the $\text{FeCl}_2(\text{PMe}_3)_2$ /potassium 2,4-dimethylpentadienide-tetrahydrofuran reaction system. Reaction a involves HO_3SCF_3 and 2 equiv of PMe_3 in diethyl ether.

Scheme II



$(\text{PMe}_3)_2$ ratio to 1:2 directs the reaction into the third manifold, shown at right in Figure 1, producing $(\eta^5\text{-}2,4\text{-Me}_2\text{pd})\text{Fe}(\text{PMe}_3)_3 + \text{FeCl}_3(\text{PMe}_3)^-$ (**3**). The third manifold is strongly favored under conditions of high absolute reagent concentrations.

B. Mechanism of Formation of Compound 1. Our proposed mechanism for the formation of **1** is presented in Scheme I. Two 2,4-dimethylpentadienide anions displace two chlorides from $\text{FeCl}_2(\text{PMe}_3)_2$ to produce $(\eta^3\text{-}2,4\text{-Me}_2\text{pd})_2\text{Fe}(\text{PMe}_3)_2$ (**A**, Scheme I). Intermediate **A** is analogous to $(\eta^3\text{-pd})_2\text{Fe}(\text{PMe}_3)_2$, the species which we have isolated and structurally characterized in the $\text{FeCl}_2\text{-}(\text{PMe}_3)_2/\text{K}^+\text{pd}^-$ reaction system.^{1b,8} However, **A** is unstable, probably as a result of unfavorable steric interactions; it loses a PMe_3 ligand and coordinates the double bond of a 2,4- Me_2pd ligand, yielding the observed product **1**.

Although the geometry of the $\eta^3\text{-}2,4\text{-Me}_2\text{pd}$ ligand cannot be definitively established in the absence of an X-ray crystal structure, the ^1H NMR spectrum of **1** supports the W-shaped geometry shown in Scheme I.⁹ In particular, H3 is highly shielded (δ 0.44), strongly suggesting that it resides inside the "mouth" of the $\eta^3\text{-}2,4\text{-Me}_2\text{pd}$ ligand (anti to the methyl group on C2). If the $\eta^3\text{-}2,4\text{-Me}_2\text{pd}$ ligand were U-shaped, H3 would reside outside the 2,4- Me_2pd "mouth" (syn to the methyl group on C2) and would be expected to exhibit a substantially lower field chemical shift (at least as low as H1_{syn} , which resonates at δ 1.06).

Recently, we have obtained the X-ray crystal structure of the related compound $(\eta^5\text{-pd})(\eta^3\text{-pd})\text{Fe}(\text{PEt}_2)_2$,¹⁰ and, in fact, it exhibits a W-shaped $\eta^3\text{-pd}$ ligand geometry.¹¹ Furthermore, the ^1H NMR spectrum of this compound closely resembles that of **1**. In particular, H3 resonates at δ 0.76, while H1_{anti} and H1_{syn} appear at δ -0.45 and 1.46, respectively.

(8) In $(\eta^3\text{-pd})_2\text{Fe}(\text{PMe}_3)_2$, the $\eta^3\text{-pd}$ ligands are bonded to iron in the syn (W-shaped) mode. The bonding modes for the $\eta^3\text{-}2,4\text{-Me}_2\text{pd}$ ligands in intermediate **A**, Scheme I, are unknown.

(9) An exo rotational orientation of the $\eta^3\text{-}2,4\text{-Me}_2\text{pd}$ ligand ("mouth" pointing away from the $\eta^5\text{-}2,4\text{-Me}_2\text{pd}$ ligand), as shown in Scheme I, is anticipated on steric grounds: Fish, R. W.; Giering, W. P.; Marten, D.; Rosenblum, M. J. *Organomet. Chem.* 1976, 105, 101.

(10) Bleeke, J. R.; Hays, M. K.; Wittenbrink, R. J., manuscript in preparation.

(11) An exo rotational orientation of the $\eta^3\text{-pentadienyl}$ ligand is observed.

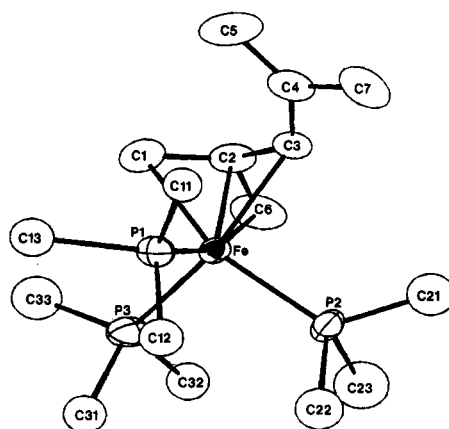


Figure 2. ORTEP drawing of (isopropenyltrimethylenemethyl)- $\text{Fe}(\text{PMe}_3)_3$ (**2**). Thermal ellipsoids are drawn to encompass 25% of the electron density. The carbon atoms of the PMe_3 ligands exhibit twofold disorder in the solid state, and one set has been omitted for clarity.

Table I. Positional Parameters with Estimated Standard Deviations for Non-Hydrogen Atoms in $(\eta^4\text{-Isopropenyltrimethylenemethyl})\text{Fe}(\text{PMe}_3)_3$ (**2**)^a

atom	x	y	z
Fe	0.2669 (1)	0.14309 (6)	0.24070 (5)
P1	0.3780 (2)	0.0986 (2)	0.1431 (1)
P2	0.1460 (2)	0.0174 (1)	0.2590 (1)
P3	0.4666 (3)	0.1258 (2)	0.3421 (1)
C1	0.305 (1)	0.2827 (5)	0.2233 (7)
C2	0.1585 (9)	0.2569 (5)	0.2337 (5)
C3	0.0583 (7)	0.2138 (5)	0.1680 (4)
C4	0.0204 (9)	0.2386 (6)	0.0810 (5)
C5	0.073 (1)	0.3130 (7)	0.0489 (6)
C6	0.153 (1)	0.2260 (6)	0.3127 (5)
C7	-0.092 (1)	0.1790 (9)	0.0269 (6)
C11	0.290 (2)	0.110 (1)	0.0323 (9)
C12	0.445 (2)	-0.023 (1)	0.137 (1)
C13	0.567 (2)	0.156 (1)	0.141 (1)
C21	-0.042 (2)	-0.004 (2)	0.210 (1)
C22	0.235 (2)	-0.101 (2)	0.244 (1)
C23	0.129 (3)	-0.003 (2)	0.370 (2)
C31	0.608 (2)	0.035 (1)	0.351 (1)
C32	0.399 (2)	0.105 (1)	0.445 (1)
C33	0.581 (2)	0.224 (2)	0.379 (1)

^a The carbon atoms of the PMe_3 ligands exhibit twofold disorder in the solid state. Only one set of phosphine carbon atom positions are included in this table. The other set of positions is available in supplementary material.

C. Mechanism of Formation of Compound 2. The 1:1 stoichiometry of the reagents in the central manifold (Figure 1) suggests that it involves a *monopentadienyl*-iron complex, perhaps $(\eta^5\text{-}2,4\text{-Me}_2\text{pd})\text{Fe}(\text{PMe}_3)_2\text{Cl}$, as an intermediate. We propose that this species then decomposes via a bimolecular disproportionation as shown in Scheme II.

In support of this mechanism, we have found that (a) 2,4-dimethylpentadiene is released as a product in this reaction¹² and (b) the yield of **2** is never greater than 50%, based on iron. Furthermore, compound **1** is definitely *not* an intermediate in the production of **2** because **1** does not react with excess PMe_3 , even at elevated temperatures.

Disproportionations similar to the one outlined in Scheme II have been previously observed (under more forcing conditions) by Impastato and Ihrman^{13a} for the

(12) Separations were performed on a 12 ft \times 1/8 in. column containing 3% OV-1 on Chrom-W-HP. An oven temperature of 70 $^\circ\text{C}$ and a carrier gas flow rate of 20 mL/min were used.

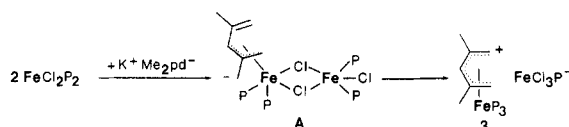
(13) (a) Impastato, F. J.; Ihrman, K. G. *J. Am. Chem. Soc.* 1961, 83, 3726. (b) Ehrlich, K.; Emerson, G. F. *Ibid.* 1972, 94, 2464.

Table II. Selected Bond Distances (Å) and Bond Angles (deg) with Estimated Standard Deviations for Compound 2

Bond Distances					
Fe-P1	2.183 (1)	Fe-C3	2.235 (5)	C2-C6	1.405 (9)
Fe-P2	2.195 (1)	Fe-C6	2.119 (6)	C3-C4	1.461 (8)
Fe-P3	2.179 (2)	C1-C2	1.405 (9)	C4-C5	1.35 (1)
Fe-C1	2.115 (6)	C2-C3	1.402 (8)	C4-C7	1.48 (1)
Fe-C2	1.924 (5)				

Bond Angles					
P1-Fe-P2	99.56 (7)	P2-Fe-C6	95.7 (3)	C3-Fe-C6	66.3 (2)
P1-Fe-P3	96.89 (7)	P3-Fe-C1	95.3 (2)	C1-C2-C3	118.1 (6)
P2-Fe-P3	97.60 (7)	P3-Fe-C2	117.3 (2)	C1-C2-C6	115.4 (7)
P1-Fe-C1	94.4 (2)	P3-Fe-C3	155.6 (2)	C3-C2-C6	116.1 (6)
P1-Fe-C2	121.2 (2)	P3-Fe-C6	92.0 (2)	C2-C3-C4	129.1 (6)
P1-Fe-C3	101.0 (2)	C1-Fe-C2	40.3 (3)	C3-C4-C5	124.9 (8)
P1-Fe-C6	161.2 (2)	C1-Fe-C3	67.1 (2)	C3-C4-C7	115.8 (7)
P2-Fe-C1	159.7 (2)	C1-Fe-C6	68.2 (3)	C5-C4-C7	119.1 (7)
P2-Fe-C2	119.4 (2)	C2-Fe-C3	38.5 (2)		
P2-Fe-C3	95.6 (2)	C2-Fe-C6	40.3 (3)		

Scheme III



formation of $(\eta^4\text{-butadiene})\text{Fe}(\text{CO})_3$ from $(\eta^3\text{-1-methylallyl})\text{Fe}(\text{CO})_3\text{Cl}$ and by Ehrlich and Emerson^{13b} for the formation of $(\eta^4\text{-trimethylenemethyl})\text{Fe}(\text{CO})_3$ from $(\eta^3\text{-2-methylallyl})\text{Fe}(\text{CO})_3\text{Cl}$.

D. X-ray Crystal Structure of 2. An ORTEP drawing of the molecular structure of 2, based on a single crystal X-ray diffraction study is shown in Figure 2. Positional parameters of non-hydrogen atoms are listed in Table I, while selected bond distances and angles are given in Table II. The complex assumes an approximate octahedral geometry with C1, C3, and C6 of the iTMM ligand and the three phosphine phosphorus atoms occupying the six coordination sites. The iTMM ligand exhibits the umbrella shape that is common among trimethylenemethyl ligands;¹⁴ C2 is 0.27 Å out of the C1/C3/C6 plane in the direction opposite the iron atom. The isopropenyl group (C4, C5, C7) is bent and twisted out of the C1/C3/C6 plane. Hence, C4 and C5 are 0.35 and 1.07 Å, respectively, out of the C1/C3/C6 plane in the direction away from iron while C7 is 0.07 Å out of the plane toward iron. The dihedral angle between planes C1/C3/C6 and C4/C5/C7 is 32°.

E. Mechanism of Formation of Compound 3. The third manifold, shown at the right in Figure 1, involves the intermediacy of a temperature-sensitive purple complex, which reacts further to produce $(\eta^5\text{-2,4-Me}_2\text{pd})\text{Fe}(\text{PMe}_3)_3^+\text{FeCl}_3(\text{PMe}_3)^-$ (3). Since this manifold is favored when the ratio of $\text{K}^+\text{2,4-Me}_2\text{pd}^-:\text{FeCl}_2(\text{PMe}_3)_2$ is 1:2 and the absolute reagent concentrations are high, we postulate that the purple intermediate is an iron dimer containing just one 2,4-Me₂pd ligand. One possible structure for the purple intermediate is shown (A, Scheme III). Note that A has the same empirical formula as 3; hence only a simple scrambling of ligands is required to convert A to 3.

F. X-ray Crystal Structure of 3. ORTEP drawings of the cation and anion of 3, based on a single-crystal X-ray diffraction study, appear in Figures 3 and 4, respectively. Positional parameters for non-hydrogen atoms are listed in Table III, while selected bond distances and angles are

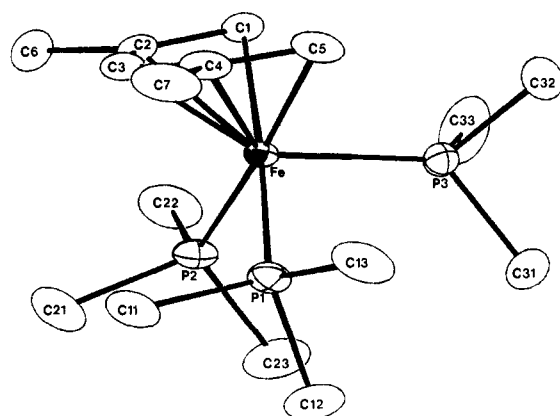


Figure 3. ORTEP drawing of $(\eta^5\text{-2,4-dimethylpentadienyl})\text{Fe}(\text{PMe}_3)_3^+$, the cation in compound 3. Thermal ellipsoids are drawn to encompass 25% of the electron density.

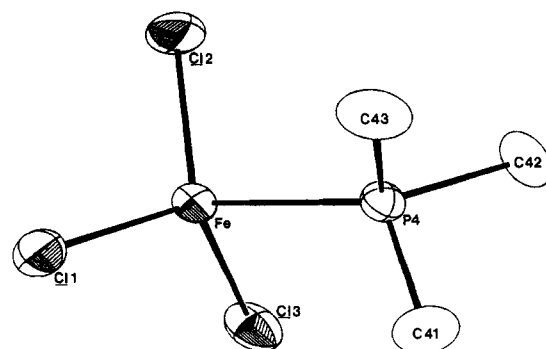


Figure 4. ORTEP drawing of $\text{FeCl}_3(\text{PMe}_3)_3^-$, the anion in compound 3. Thermal ellipsoids are drawn to encompass 25% of the electron density.

given in Table IV. The cation assumes an approximate octahedral geometry with C1, C3, and C5 of the 2,4-Me₂pd ligand and the three phosphine phosphorus atoms occupying the six coordination sites. Phosphorus atom P3 is bent up into the mouth of the 2,4-Me₂pd ligand; hence P3 is 2.091 Å from the pentadienyl plane, while P1 and P2 are 3.040 and 3.046 Å away, respectively.¹⁵ The anion exhibits an ethane-like geometry, with the three chloro groups on Fe2 and the three methyl groups on P4 arranged in a staggered orientation.

G. Synthesis, Mechanism of Formation, and Solution Dynamics of $(\eta^5\text{-2,4-Dimethylpentadienyl})\text{Fe}$

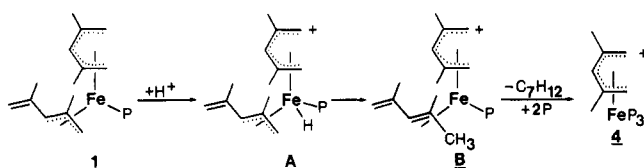
(14) (a) Deeming, A. J. In *Comprehensive Organometallic Chemistry*; Wilkinson, G., Stone, F. G. A., Abel, E. W., Eds.; Pergamon: Oxford, 1982; Vol. 4, p 462. (b) Grosselin, J.-M.; LeBozec, H.; Moinet, C.; Toupet, L.; Dixneuf, P. H. *J. Am. Chem. Soc.* 1985, 107, 2809.

(15) We have observed analogous bending of the "mouth" phosphines in the structures of several $(\eta^5\text{-pd})\text{MnP}_3$ and $(\eta^5\text{-pd})\text{ReP}_3$ complexes (see ref 1f.g).

Table III. Positional Parameters with Estimated Standard Deviations for Non-Hydrogen Atoms in (η^5 -2,4-Dimethylpentadienyl)Fe(PMe₃)₃⁺FeCl₂(PMe₃)₃⁻ (3)

atom	x	y	z
Fe1	0.46991 (3)	0.21220 (3)	0.03857 (3)
P1	0.58633 (7)	0.20443 (8)	0.00100 (8)
P2	0.42854 (7)	0.17841 (8)	-0.07750 (7)
P3	0.45323 (8)	0.33098 (7)	0.02075 (9)
C1	0.3627 (3)	0.2114 (3)	0.0852 (3)
C2	0.3894 (3)	0.1395 (3)	0.0843 (3)
C3	0.4583 (3)	0.1207 (3)	0.1128 (3)
C4	0.5101 (3)	0.1671 (3)	0.1457 (3)
C5	0.4992 (3)	0.2410 (3)	0.1539 (3)
C6	0.3421 (3)	0.0787 (3)	0.0541 (4)
C7	0.5800 (4)	0.1321 (4)	0.1754 (4)
C11	0.6233 (3)	0.1116 (3)	-0.0021 (4)
C12	0.6177 (3)	0.2330 (4)	-0.0920 (4)
C13	0.6535 (3)	0.2548 (4)	0.0565 (4)
C21	0.4560 (3)	0.0880 (3)	-0.1086 (4)
C22	0.3300 (3)	0.1748 (4)	-0.0978 (4)
C23	0.4480 (4)	0.2319 (5)	-0.1611 (4)
C31	0.5088 (4)	0.3827 (3)	-0.0442 (4)
C32	0.4648 (5)	0.3920 (4)	0.1006 (4)
C33	0.3631 (4)	0.3582 (4)	-0.0105 (6)
Fe2	0.23082 (4)	0.07079 (4)	0.69239 (4)
Cl1	0.1849 (1)	0.04763 (9)	0.57499 (9)
Cl2	0.1799 (1)	0.1670 (1)	0.7507 (1)
Cl3	0.35404 (8)	0.0637 (1)	0.70976 (9)
P4	0.19431 (8)	-0.03594 (8)	0.76227 (8)
C41	0.2310 (4)	-0.1217 (4)	0.7306 (5)
C42	0.2193 (4)	-0.0338 (5)	0.8613 (4)
C43	0.0980 (4)	-0.0529 (5)	0.7607 (5)

Scheme IV



(PMe₃)₃O₃SCF₃⁻ (4). The reaction of 1 with HO₃SCF₃ and additional PMe₃ in diethyl ether produces (η^5 -2,4-Me₂pd)Fe(PMe₃)₃⁺O₃SCF₃⁻ (4).¹⁶ We propose that this reaction involves protonation of the iron center followed by rapid migration of the hydrogen ligand to C1 of the η^3 -2,4-Me₂pd ligand. The resulting diene ligand is then displaced by two PMe₃ molecules (see Scheme IV).¹⁷ In order to minimize the side reaction between HO₃SCF₃ and free PMe₃, the acid is added to 1 first, and the resulting solution is stirred for 10 min at -78 °C before addition of the phosphine reagent (see E in the Experimental Section). However, this side reaction cannot be completely eliminated, and 4 is typically contaminated with ~20% (by weight) of the phosphonium salt HPMe₃⁺O₃SCF₃⁻. Neither repeated recrystallization nor column chromatography has led to a clean separation of the two components.

In solution at 25 °C, the η^5 -2,4-Me₂pd ligand in 4 rotates with respect to the Fe(PMe₃)₃ fragment, exchanging the three phosphine ligands.¹⁸ Hence, the room-temperature ³¹P{¹H} NMR spectrum consists of a single peak. However, as the sample is cooled to -30 °C, this rotational process is slowed and the ³¹P{¹H} NMR signal splits into two peaks, one of intensity 2 due to phosphines under the edges of the 2,4-Me₂pd ligand and the other of intensity 1 due to

(16) Recently, we have observed similar acid cleavages of η^5 -penta-dienyl ligands in the reactions of (η^5 -pd)₂Fe(PMe₃)₂ and (η^5 -pd)(η^3 -pd)-Fe(PEt₃) with HO₃SCF₃ (ref 10).

(17) In support of this mechanism we have found that 1 equiv of 2,4-dimethylpentadiene is released in the reaction (see ref 12 for gas chromatographic separation conditions).

(18) We have observed analogous rotations in several (η^5 -pd)MnP₃ and (η^5 -pd)ReP₃ complexes (ref 1f,g).

the "mouth" phosphine. Line-shape simulations of the variable-temperature ³¹P{¹H} spectra have enabled us to calculate a ΔG^\ddagger for the rotational process of 11.5 ± 0.5 kcal.

Experimental Section

A. General Comments. All manipulations were carried out under inert atmosphere by using either drybox or Schlenk techniques. Tetrahydrofuran and diethyl ether were dried with sodium/benzophenone and distilled before use. Pentane was dried over calcium hydride and distilled. Methylene chloride was degassed. Anhydrous iron(II) chloride (Thiokol, Alfa), trifluoromethanesulfonic acid (Aldrich), 2,4-dimethylpentadiene (Wiley), and trimethylphosphine (Strem) were all used without further purification.

NMR experiments were performed on a Varian XL-300 NMR spectrometer. ¹H (300-MHz) and ¹³C (75-MHz) spectra were referenced to tetramethylsilane. ³¹P spectra (121 MHz) were referenced to external H₃PO₄.¹⁹ In general, ¹³C NMR peak assignments were made from gated decoupled spectra. ¹H NMR peak assignments were then obtained from ¹³C-¹H shift-correlated (HETCOR) 2D spectra. Some connectivities were ascertained from ¹H-¹H shift-correlated (COSY) 2D spectra. Infrared spectra were recorded on a Perkin-Elmer 283B spectrophotometer. Microanalyses were performed by Galbraith Laboratories, Inc., Knoxville, TN, or Schwarzkopf Microanalytic Laboratory, Inc., Woodside, NY.

B. Synthesis of (η^5 -2,4-Dimethylpentadienyl)(η^3 -2,4-dimethylpentadienyl)Fe(PMe₃) (1). FeCl₂ (1.9 g, 1.5×10^{-2} mol) and PMe₃ (2.3 g, 3.0×10^{-2} mol) were refluxed in 200 mL of tetrahydrofuran for 1 h to form a pale green solution of FeCl₂(PMe₃)₂.⁶ This solution was cooled to -78 °C, and potassium 2,4-dimethylpentadienide-tetrahydrofuran⁷ (6.2 g, 3.0×10^{-2} mol) in 200 mL of tetrahydrofuran was added over a period of 30 min. The resulting dark reddish brown solution was stirred for 2 h while being warmed to room temperature, filtered through Celite, and evaporated to dryness. The dark red product was extracted with pentane and crystallized at -30 °C: yield of crude product 4.4 g (90%); yield of crystallized product 2.9 g (60%). Anal. Calcd for C₁₇H₃₁FeP: C, 63.35; H, 9.71. Found: C, 62.78; H, 9.42. ¹³C{¹H} NMR (benzene-d₆, 20 °C): δ 147.6 (C4 of η^3), 108.4 (C5 of η^3), 98.9 (C3 of η^5), 98.5 (C4 of η^5), 97.7 (C2 of η^5), 89.5 (C2 of η^3), 53.0 (C3 of η^3), 48.4 (C5 of η^5 , d, J_{C-P} = 15 Hz), 47.4 (C1 of η^5 , d, J_{C-P} = 17 Hz), 39.6 (C1 of η^3), 27.2, 25.2, 25.0, 23.9 (methyl groups of 2,4-Me₂pd's), 20.0 (PMe₃, d, J_{C-P} = 23 Hz). ¹H NMR (benzene-d₆, 20 °C): δ 5.25 (H5 of η^3 , 1, s), 5.07 (H5 of η^3 , 1, s), 4.46 (H3 of η^5 , 1, s), 2.47 (H5_{syn} of η^5 , 1, d, J_{H-P} = 6.3 Hz), 2.31 (methyl group of η^3 , 3, s), 1.95 (H1_{syn} of η^5 , 1, d, J_{H-P} = 8.0 Hz), 1.87, 1.86 (methyl groups of η^5 , 6, s's), 1.71 (methyl group of η^3 , 3, s), 1.21 (PMe₃, 9, d, J_{H-P} = 7.8 Hz), 1.06 (H1 of η^3 , 1, s), 0.44 (H3 of η^3 , 1, d, J_{H-P} = 11.4 Hz), -0.56 (H1 of η^3 , 1, d, J_{H-P} = 16.8 Hz), -0.11 (H5_{anti} of η^5 , 1, d, J_{H-P} = 7.8 Hz), -1.20 (H1_{anti} of η^5 , 1, d, J_{H-P} = 7.8 Hz). ³¹P{¹H} NMR (benzene-d₆, 20 °C): δ 26.4 (sharp singlet). IR (pentane): 3200-2800 (s, 2,4-Me₂pd/PMe₃), 1604 (m, C=C of η^3), 1460-1440, 1380 (s, 2,4-Me₂pd/PMe₃), 954, 934 cm⁻¹ (s, PMe₃).

C. Synthesis of (η^4 -Isopropenyltrimethylenemethyl)Fe(PMe₃)₃ (2). FeCl₂ (1.9 g, 1.5×10^{-2} mol) and PMe₃ (2.3 g, 3.0×10^{-2} mol) were refluxed in 200 mL of tetrahydrofuran for 1 h to form a pale green solution of FeCl₂(PMe₃)₂.⁶ This solution was cooled to -78 °C, and potassium 2,4-dimethylpentadienide-tetrahydrofuran⁷ (4.1 g, 2.0×10^{-2} mol) in 200 mL of tetrahydrofuran was added over a period of 30 min. The resulting dark reddish brown solution was stirred for 15 min at -78 °C and for 2 h while being warmed to room temperature. It was then filtered through Celite and evaporated to dryness. The dark red product was extracted with pentane and crystallized at -30 °C: yield of crude product 2.7 g (48%); yield of crystallized product 1.8 g (32%). Crude 2 was always contaminated with a small quantity of 1 but could be purified by repeated crystallization from pentane. Anal. Calcd for C₁₆H₂₇FeP₃: C, 50.80; H, 9.88. Found: C, 50.37; H, 9.84. ¹³C{¹H} NMR (benzene-d₆, 20 °C): δ 150.6 (C4), 105.0 (C5), 104.8 (C2), 62.3 (C3, q, J_{C-P} = 7 Hz), 42.0 (C1, C6, m), 27.2 (C7), 24.3 (PMe₃, d, J_{C-P} = 19 Hz), 23.4 (PMe₃, d, J_{C-P} = 19 Hz), 22.6 (PMe₃, d, J_{C-P} = 18 Hz). ¹H NMR (benzene-d₆, 20 °C): δ 5.47 (H5, 1,

(19) PMe₃ resonates 62 ppm upfield from H₃PO₄.

Table IV. Selected Bond Distances (Å) and Bond Angles (deg) with Estimated Standard Deviations for Compound 3

cation		anion	
Bond Distances			
Fe1-P1	2.275 (1)	Fe1-C5	2.179 (4)
Fe1-P2	2.274 (1)	C1-C2	1.414 (6)
Fe1-P3	2.232 (1)	C2-C3	1.398 (7)
Fe1-C1	2.171 (4)	C2-C6	1.508 (7)
Fe1-C2	2.179 (4)	C3-C4	1.397 (7)
Fe1-C3	2.161 (4)	C4-C5	1.385 (7)
Fe1-C4	2.195 (4)	C4-C7	1.521 (7)
Bond Angles			
P1-Fe1-P2	90.30 (5)	P3-Fe1-C5	85.7 (1)
P1-Fe1-P3	98.43 (5)	C1-Fe1-C3	69.5 (2)
P2-Fe1-P3	95.62 (5)	C1-Fe1-C5	80.7 (2)
P1-Fe1-C1	173.3 (1)	C3-Fe1-C5	68.6 (2)
P1-Fe1-C3	104.2 (1)	C1-C2-C3	122.7 (4)
P1-Fe1-C5	95.0 (1)	C1-C2-C6	120.3 (5)
P2-Fe1-C1	93.8 (1)	C3-C2-C6	117.0 (4)
P2-Fe1-C3	108.0 (1)	C2-C3-C4	127.1 (4)
P2-Fe1-C5	174.3 (1)	C3-C4-C5	123.1 (4)
P3-Fe1-C1	86.5 (1)	C3-C4-C7	116.5 (5)
P3-Fe1-C3	146.8 (1)	C5-C4-C7	120.4 (5)
C1-Fe2-Cl1	114.92 (6)		
C1-Fe2-Cl3	116.90 (6)		
Cl2-Fe2-Cl3	113.93 (7)		
Cl1-Fe2-P4	102.73 (6)		
Cl2-Fe2-P4	105.63 (6)		
Cl3-Fe2-P4	100.02 (6)		

s), 4.86 (H5, 1, s), 2.05 (H1 or H6, 1, d of d, $J_{P-H} = 12$ Hz, $J = 4$ Hz), 1.95 (CH₃, 3, s), 1.90 (H3, 1, s), 1.16 (PMe₃, 9, d, $J_{H-P} = 6$ Hz), 1.07 (PMe₃, 9, d, $J_{H-P} = 6$ Hz), 1.00 (H1 or H6, 1, partially obscured), 0.90 (PMe₃, 9, d, $J_{H-P} = 6$ Hz), 0.70 (H1 or H6, 1, d of d, $J_{P-H} = 12$ Hz, $J = 4$ Hz), 0.60 (H1 or H6, 1, d, $J_{P-H} = 12$ Hz). ³¹P{¹H} NMR (benzene-*d*₆, 20 °C): δ 31.65 (t, $J_{P-P} = 13$ Hz), 24.4 (t, $J_{P-P} = 13$ Hz), 20.2 (t, $J_{P-P} = 13$ Hz). IR (pentane): 3200–2800 (s, iTMM/PMe₃), 1603 (m, isopropenyl C=C), 1425, 1290, 1275 (s, iTMM/PMe₃), 945, 930 cm⁻¹ (vs, PMe₃).

D. Synthesis of (η⁵-2,4-Dimethylpentadienyl)Fe(PMe₃)₃⁺FeCl₃(PMe₃)⁻ (3). FeCl₂ (1.9 g, 1.5 × 10⁻² mmol) and PMe₃ (2.3 g, 3.0 × 10⁻² mol) were refluxed in 100 mL of tetrahydrofuran for 1 h to form a pale green solution of FeCl₂(PMe₃)₂.⁶ This solution was cooled to -78 °C, and potassium 2,4-dimethylpentadienide-tetrahydrofuran⁷ (1.6 g, 7.8 × 10⁻³ mol) in 60 mL of tetrahydrofuran was then added dropwise over a period of 30 min. The resulting dark purple solution was stirred at -78 °C for 1 h, filtered through Celite while still cold, and evaporated to dryness. Addition of pentane to the residue yielded 3 as an orange powder; yield 3.3 g (71%). Anal. Calcd for C₁₉H₄₇Fe₂Cl₃P₄: C, 36.95; H, 7.69. Found: C, 36.35; H, 7.47. ¹³C and ¹H NMR signals were very broad, probably due to the presence of the paramagnetic anion. ³¹P{¹H} NMR (methylene-*d*₂ chloride, -50 °C/stopped exchange): δ 19.4 (PMe₃ under "mouth"), 13.4 (PMe₃'s under edges). Temperature-dependent behavior similar to that described for 4 (vide infra) was observed. IR (methylene chloride): 3030–2965 (w, 2,4-Me₂pd/PMe₃), 1420, 1310–1257 (m, 2,4-Me₂Pd/PMe₃), 952, 947 cm⁻¹ (s, PMe₃).

E. Synthesis of (η⁵-2,4-Dimethylpentadienyl)Fe(PMe₃)₃⁺O₃SCF₃⁻ (4). Trifluoromethanesulfonic acid (0.30 g, 2.0 × 10⁻³ mol) in 25 mL of diethyl ether was added dropwise over 10 min to a cold (-78 °C), stirred solution of (η⁵-2,4-dimethylpentadienyl)(η³-2,4-dimethylpentadienyl)Fe(PMe₃) (0.61 g, 2.0 × 10⁻³ mol) in 75 mL of diethyl ether. The resulting solution was stirred at -78 °C for 10 min before adding PMe₃ (0.78 g, 1.0 × 10⁻² mol) in 25 mL diethyl ether and stirring for an additional 45 min at -78 °C. The solution was then allowed to warm to room temperature, causing its color to lighten gradually and a mixture of 4 and HPMe₃⁺O₃SCF₃⁻ to precipitate as an orange powder. Quantitative ¹H and ³¹P NMR experiments showed the powder to contain 4 and HPMe₃⁺O₃SCF₃⁻ in a 63:37 molar ratio (or 80:20 weight ratio). Attempts to separate the two components by recrystallization and column chromatography were unsuccessful; total yield of 4 plus HPMe₃⁺O₃SCF₃⁻ 0.97 g; yield of 4 0.78 g (74%). Anal. Calcd for 80:20 mixture (by weight) of 4 (C₁₇H₃₆FeP₃O₃SF₃) and HPMe₃⁺O₃SCF₃⁻ (C₄H₁₀PO₃SF₃): C, 35.16; H, 6.70. Found: C, 35.13; H, 6.72.

Characterization of HPMe₃⁺O₃SCF₃⁻. ¹³C{¹H} NMR (methylene-*d*₂ chloride, 20 °C): δ 122.1 (O₃SCF₃⁻, q, $J_{C-F} = 330$ Hz), 5.29 (HPMe₃⁺, d, $J_{C-P} = 56$ Hz). ¹H NMR (methylene-*d*₂ chloride, 20 °C): δ 1.80 (methyl H's, d of d, $J_{H-P} = 15$ Hz, J_{H-H}

= 5.5 Hz). ³¹P{¹H} NMR (methylene-*d*₂ chloride, 20 °C): δ 2.71 (s).

Characterization of 4. ¹³C{¹H} NMR (methylene-*d*₂ chloride, 20 °C): δ 122.1 (O₃SCF₃⁻, q, $J_{C-F} = 330$ Hz), 112.8 (C2/C4), 89.0 (C3), 49.8 (C1/C5), 25.3 (PMe₃ under 2,4-Me₂pd "mouth"), 22.6 (PMe₃'s under 2,4-Me₂pd edges). ¹H NMR (methylene-*d*₂ chloride, 20 °C): δ 5.65 (H3, 1, s), 2.20 (2,4-Me₂pd methyl H's, 6, s), 1.80 (H1_{syn}/H5_{syn}, 2, s), 1.35 (PMe₃ H's, 27, s), -0.49 (H1_{anti}/H5_{anti}, 2, s). ³¹P{¹H} NMR (methylene-*d*₂ chloride, -50 °C/stopped exchange): δ 19.4 (PMe₃ under "mouth"), 13.4 (PMe₃'s under edges). The ³¹P{¹H} NMR signals coalesced to a single peak (δ 15.4) at 25 °C. IR (methylene chloride): 3145–2915 (w, 2,4-Me₂pd/PMe₃), 1418, 1263, 1221 (s, 2,4-Me₂pd/PMe₃), 1152, 1028 (s, O₃SCF₃⁻), 934, 959 cm⁻¹ (s, PMe₃).

F. X-ray Diffraction Studies of 2 and 3. Single crystals of 2 suitable for X-ray diffraction were grown from a saturated pentane solution; those of 3 were obtained from tetrahydrofuran. Data were collected at room temperature on a Nicolet P3 diffractometer, using graphite-monochromated Mo Kα radiation. All data reduction and structure refinement were done by using the Enraf-Nonius structure determination package on a VAX 11/780 computer (modified by B.A. Frenz and Assoc., Inc., College Station, TX).²⁰ Crystal data and details of data collection and structure analysis are summarized in Table V.

The structure of 2 was solved by standard Fourier techniques following the location of the iron atom from a Patterson map. Each of the nine PMe₃ carbon atoms exhibited a twofold disorder which we were able to model. For each PMe₃ ligand, the two sets of equally populated²¹ carbon atom positions were related by a rotation of ~30° around the Fe–P vector (range of rotations, 18.9–43.0°; average rotation, 31.7°). The disordered phosphine carbon atoms were refined isotropically, while all other non-hydrogen atoms in the molecule were refined anisotropically. Hydrogen atoms on the 2,4-Me₂pd ligand were added at idealized positions riding upon their respective carbon atoms and were included in structure factor calculations but not refined. Hydrogens on the disordered phosphine carbons were not included.

The structure of 3 was solved by direct methods (MULTAN). All of the non-hydrogen atoms were refined with anisotropic thermal parameters. The hydrogen atoms were added at idealized positions riding upon their respective carbon atoms and were included in the structure factor calculations but not refined.

G. Dynamic NMR Studies. Samples were dissolved in methylene-*d*₂ chloride, and NMR spectra were recorded over the temperature range -50 to +30 °C. Probe temperatures were

(20) Atomic scattering factors were obtained from: *International Tables for X-Ray Crystallography*; Kynoch Press: Birmingham, England, 1974; Vol. IV.

(21) The site occupancy factor of 0.5 was estimated from electron densities.

Table V. Crystal and Diffraction Data for (η^4 -Isopropenyltrimethylenemethyl)Fe(PMe₃)₃ (2) and (η^5 -2,4-Dimethylpentadienyl)Fe(PMe₃)₃⁺FeCl₃(PMe₃)₃⁻ (3)

	2	3
formula	C ₁₈ H ₃₇ FeP ₃	C ₁₉ H ₃₇ Fe ₂ Cl ₃ P ₄
mol wt	378.29	617.59
space group	P2 ₁ /c ^a	C2/c ^b
a, Å	8.878 (1)	18.442 (5)
b, Å	14.737 (4)	18.433 (5)
c, Å	16.689 (3)	17.875 (5)
β , deg	102.25 (1)	91.87 (2)
V, Å ³	2129.5 (8)	6073 (3)
Z	4	8
cryst color	red	orange
cryst dimens, mm	0.6 × 0.4 × 0.3	0.5 × 0.3 × 0.3
d _{calcd} , g/cm ³	1.180	1.351
radiation, Å	Mo K α , λ = 0.71069	Mo K α , λ = 0.71069
μ _{calcd} , cm ⁻¹	8.543	14.368
abs corr	none	none
scan type	ω	ω
scan rate, deg/min	variable, 2-29	variable, 4-29
2 θ min, deg	3	3
2 θ max, deg	50	50
octant collected	<i>h, k, ±l</i>	<i>h, k, ±l</i>
no. of unique data collected	3444	5335
no. of data with $I > 3\sigma(I)$	2270	3531
agreement between equiv reflects (R_{merge}) ^c	0.034	0.045
no. of parameters varied	172	253
data/parameter ratio	13.20	13.96
final R_F ^d	0.063	0.048
final R_{wF} ^e	0.093	0.066
largest peak in final diff Fourier map, e/Å ³	0.62	0.47

^a Uniquely determined from systematic absences ($0k0$, $k = 2n + 1$; $h0l$, $l = 2n + 1$). ^b Systematic absences (hkl , $h + k = 2n + 1$; $h0l$, $l = 2n + 1$) indicated space group Cc or $C2/c$. The centrosymmetric space group was suggested by statistical tests and confirmed by successful refinement. ^c $R_{\text{merge}} = \sum |F - F_{\text{av}}| / \sum |F_{\text{av}}|$. ^d $R_F = \sum ||F_o| - |F_c|| / \sum |F_o|$. ^e $R_{wF} = [\sum w(|F_o| - |F_c|)^2 / \sum w|F_o|^2]^{1/2}$; $w = 1 / \sigma^2(|F_o|)$.

calibrated by using the temperature dependence of the difference in chemical shift between the ¹H resonances of the methyl and hydroxyl groups of methanol below ambient temperatures and between the ¹H resonances of the methylene and hydroxyl groups of ethylene glycol above ambient temperatures.²² Theoretical lineshapes were calculated for a series of rates by using the method of C. S. Johnson.^{23,24} The experimental spectra (measured at various temperatures) were matched against the theoretical spectra, and, in this way, exchange rate constants were determined for each temperature. These exchange rate constants, k , were then used to calculate the free energy of activation, ΔG^\ddagger , at each temperature, T , by using the Eyring equation $k = (k'/h)Te^{-\Delta G^\ddagger/RT}$, where k' = Boltzmann's constant, h = Planck's constant, and R = ideal gas constant.²⁵

(22) Von Geet, A. L. *Anal. Chem.* **1968**, *40*, 2227.

(23) Johnson, C. S., Jr. *Am. Jour. Phys.* **1967**, *35*, 929.

(24) Martin, M. L.; Martin, G. J.; Delpuech, J.-J. *Practical NMR Spectroscopy*; Heydon: London, 1980; pp 303-309.

Conclusion

The course of the reaction of FeCl₂(PMe₃)₂ with potassium 2,4-dimethylpentadienide-tetrahydrofuran (K⁺2,4-Me₂pd⁻) depends dramatically on the K⁺2,4-Me₂pd⁻:Fe ratio. When a ratio of 2:1 is employed, the mixed-mode complex (η^5 -2,4-Me₂pd)(η^3 -2,4-Me₂pd)Fe(PMe₃) (1) is generated. A 1:1 ratio of K⁺2,4-Me₂pd⁻:Fe leads to activation of a C-H bond in the 2,4-Me₂pd group and production of (η^4 -iTMM)Fe(PMe₃)₃ (2) via a bimolecular disproportionation route ("iTMM" is the isopropenyl-substituted trimethylenemethyl ligand). Use of a 1:2 K⁺2,4-Me₂pd⁻:Fe ratio produces the unusual diiron salt (η^5 -2,4-Me₂pd)Fe(PMe₃)₃⁺FeCl₃(PMe₃)₃⁻ (3).

When (η^5 -2,4-Me₂pd)(η^3 -2,4-Me₂pd)Fe(PMe₃) is protonated with HO₃SCF₃ in the presence of PMe₃, the hydrogen ligand migrates to η^3 -2,4-Me₂pd. The resulting diene ligand is then displaced by PMe₃, producing (η^5 -2,4-Me₂pd)Fe(PMe₃)₃⁺O₃SCF₃⁻ (4). Acid cleavage reactions of this type promise to provide a general route to a large class of (η^5 -2,4-Me₂pd)FeL₃⁺ complexes, and we are continuing to explore this synthetic approach. Furthermore, we have begun to prove the reactivity of cationic complex 4 toward nucleophiles. Results of this work will be reported in a future communication.

Acknowledgment. We thank the National Science Foundation (Grant CHE-8520680) and the donors of the Petroleum Research Fund, administered by the American Chemical Society, for financial support. Additional support was provided by Monsanto Co. and by BRSG S07 RR07054-20 awarded by the Biomedical Research Support Grant Program, Division of Research Resources, National Institutes of Health. NMR spectra were obtained with the assistance of Dr. André d'Avignon, director of the Washington University High Resolution NMR Service Facility. This facility was funded in part by NIH Biomedical Research Support Instrument Grant 1 S10 RR02004 and by a gift from Monsanto Co. We thank Professor G. G. Stanley and David J. Rauscher (Washington University) for assistance with the single-crystal X-ray diffraction studies of 2 and 3 and Ms. Kim Zeimet (a participant in Washington University's Summer Undergraduate Research Program) for synthetic help.

Registry No. 1, 106419-01-6; 2, 106419-02-7; 3, 106419-05-0; 4, 106419-06-1; FeCl₂(PMe₃)₃, 55853-16-2; K⁺2,4-Me₂Pd⁻, 74205-98-4; HPMe₃⁺O₃SCF₃⁻, 106419-07-2.

Supplementary Material Available: ORTEP drawing of 2 showing all non-hydrogen atoms and listings of final atomic coordinates, thermal parameters, bond lengths, bond angles, and significant least-squares planes including subtended dihedral angles for 2 and 3 (16 pages); listings of observed and calculated structure factor amplitudes for 2 and 3 (23 pages). Ordering information is given on any current masthead page.

(25) Lowry, T. H.; Richardson, K. S. *Mechanism and Theory in Organic Chemistry*; Harper and Row: New York, 1976.